ANALYSES ON SEISMIC GROUND MOTION PARAMETERS INCLUDING VERTICAL COMPONENTS

by

Yorihiko Ohsaki I, Makoto Watabe II, and Masanobu Tohdo III.

SUMMARY

The relations among various intensities of earthquake ground motions are first obtained for understanding the general characteristics of earthquake ground motions and ground motion parameters, such as the maxima and frequency characteristics, expressed in terms of magnitude of earthquake and hypocentral distance are evaluated. In addition, effective peak acceleration for engineering purpose and deterministic intensity function for the simulation of ground motions are proposed. Using these parameters, the proposal of a procedure for estimation of the design earthquake concludes this paper.

INTRODUCTION

In engineering purpose of seismic design of structures, it is essential to understand the characteristics of earthquake ground motions, such as the maxima and frequency characteristics. In view of the limitation of obtained strong motion accelerograms and the randomness of source mechanisms and paths through which seismic waves pass, the stochastic analyses based on recorded accelerograms are appropriate for the quantification of earthquake ground motion parameters for future engineering applicaitons.

It is the purpose of this paper to analyse stochastically the various parameters of earthquake ground motions by the use of accelerograms recorded in both Japan and the United States. Based on the awareness that the simultaneous response effects due to three dimensional earthquake groud motions are important factors for complex structures such as nuclear power plants, the parameters in vertical components are included in these analyses, as well. In addition, discussions on the meaning of effective peak acceleration in view of practical engineering purposes are mentioned.

RELATIONS AMONG VARIOUS PHYSICAL PARAMETERS REPRESENTING INTENSITIES OF EARTHQUAKE GROUND MOTIONS

At first, the cross correlations between the maximum values of acceleration, velocity, displacement and Housner s Spectral Intensity [1] with zero and 0.2 dampings are stochastically analysed. The results are indicated in Table 1 from which it may be suggested that measures to represent intensity of ground motions such as values mentioned above are extremely cross correlated, therefore, the choice of these measures is allowed to be

---

I Professor, Faculty of Engineering, University of Tokyo, Japan
II Director, Structural Engineering Department, Building Research Institude, Ministry of Construction, Japan
III Research Member, Structural Engineering Department, Nuclear Power Division, Toda Construction Co.Ltd., Japan

rather arbitrary. This analysis also provides linear relations between these maxima. The results are indicated in Table 2, which suggests reasonable ratios between two values of maxima such as horizontal and vertical acceleration, velocity, displacement and spectral intensity.

One example of the probability distribution of the variables of the difference between real observed data and values estimated by linear relations in logarithmic scale and their deviations are shown in Fig. 1 and Table 3, respectively. From the results, it can be regarded that the probability distribution mentioned above is similar to Gaussian distribution and the standard deviation to convert maximum velocity into spectral intensity of earthquake ground mations is about 0.15 in logarithmic scale or 1.4 in decimal scale. Therefore, in case of conservative estimation, the value by linear relation in Table 2 may be multiplied by the 1 standard deviation 1.4 with exceedence probability 16%.

MAXIMA OF EARTHQUAKE GROUND MATIONS

Maxima of earthquake ground motions on rock site

From the 75 sets of earthquakes obtained on rock site in Japan, with the parameters of magnitude of earthquake (M) and hypocentral distance (x km) shown in Fig. 2, the following equations for the relation between the hypocentral distance and the maxima of acceleration (A) and velocity (V) with the magnitude are derived by regression analysis.

$$A^h = 10^{0.440M - 1.38 \log x + 1.04} \quad \text{in cm/sec}^2 \qquad (1)$$

$$V^h = 10^{0.607M - 1.19 \log x - 1.40} \quad \text{in cm/sec} \qquad (2)$$

Where suffix h indicates a horizontal component. The equation (2) is similar to Kanai's equation of the maximum velocity [2].

While the radius (D km) of the spherical volume within which hypocenters of aftershocks of the earthquake exist can be expressed in terms of the magnitude (M) followingly [3].

$$D = 10^{0.353M - 1.134} \quad \text{in km} \qquad (3)$$

Assuming that a half of the above value D is the depth of energy release center and using Eqs. (1) and (2), the relation between the maxima and the epicentral distance can be expressed as illustrated in Figs. 3 and 4 with the parameter of magnitude. Figs. 3 and 4 suggest that the maximum probable value of acceleration on rock site will rarely exceed the value of 400 cm/sec^2 and that of velocity 50 cm/sec.

Although the number of recorded accelerograms in vertical components is limited, the equations in vertical components similar to Eqs. (1) and (2) herein dare to be obtained. The results are as follows.

$$A^v = 10^{0.485M - 1.85 \log x + 1.38} \quad \text{in cm/sec}^2 \qquad (4)$$

$$V^v = 10^{0.485M - 1.25 \log x - 0.85} \quad \text{in cm/sec} \qquad (5)$$

Where suffix v indicates a vertical component. It can be seen in the comparison between Eqs. (1), (2), (4) and (5) that the maximum acceleration in vertical component is rather fast attenuated than the other maxima as the

hypocentral distance becomes longer, and that the ratio of maximum velocity to maximum acceleration in both horizontal and vertical components with a given magnitude becomes larger as the hypocentral distance increases, on the other hand the ratio of the maxima in vertical component to horizontal component becomes smaller as the hypocentral distance becomes longer and this ratio nearly becomes 0.4– 0.6, with some exceptional cases of data in the near fields where the maximum accelerations in both vertical and horizontal components become identical.

Effective peak acceleration

The accelerogram of EW component recorded at Pacoima dam during San Fernando Earthquake (1971) shown in Fig. 5 is famous as the first record over the gravity acceleration. The peak acceleration, however, is a kind of so called "Spike" and this value will be greatly different from the value obtained by stochastic analyses as mentioned above. When considering the relation between maximum acceleration and the maximum response, the question arises, if sharp peak acceleration such as Pacoima can express the intensity scale appropriate for aseismic engineerings.

On the basis of this question, the effective peak acceleration for engineering purpose is proposed. The proposed effective peak acceleration may be defined followingly;

First, let obtain Housner's Spectral Intensity with 5% damping ratio SI. Then cut out all the acceleration value above the threshold acceleration value A_s, for which accelerogram, Housner's Spectral Intensity becomes 90% of the original SI. The final effective peak acceleration value Aep can be obtained by the equation below.

$$Aep = As \cdot 100/90 \qquad (6)$$

In this proposal, the effective peak acceleration of Pacoima is 352 cm/sec^2. Figs. 6 and 7 show the cut out accelerogram having spectral intensity 0.9 SI and the comparison of original response spectrum and that for cut out accelerogram respectively.

Table 4 presents the maximum acceleration of the original and the effective peak acceleration for four accelerograms. These values may be acceptable from engineering design point of view.

SPECTRAL CHARACTERISTICS OF EARTHQUAKE GROUND MOTIONS ON ROCK SITE

Velocity response spectrum in horizontal and vertical components

The spectral shape of accelerograms on the surface of bed-rock may be influenced by the source mechanisms of earthquakes and the formations through which seismic waves pass. The velocity response spectrum $S_V(M,X,T)$ with 5% damping ratio on free field bed-rock is assumed to be the function of magnitude M and hypocentral distance X (km) in addition to period T (sec.) as follows [4].

$$\log S_V\ (M,X,T) = A(T)M - B(T)\ \log x - C(T) \qquad \text{in cm/sec} \quad (7)$$

Using 75 accelerograms in horizontal components obtained on free field bed-rock shown in Fig. 2, coefficients A, B and C's for every period of spectral values are obtained through regression analysis. The solid lines in Fig. 8 show the resulted coefficients of A, B and C's for velocity response spectra with 5% damping ratio. The cross correlation coefficient between response spectra for observed real ones and for calculated ones using the resulted

coefficents A,B and c's is about 0.8, and the deviation coefficient between the above two spectra is about 0.5 in the almost entire period range. It should be noted that the above correlation and deviation coefficients are evaluated from the response values in logarithmic scale. The solid lines in Fig. 9 are some examples of velocity response spectra with the constant hypocentral distance 50km for the various values of magnitude. The similar examples are also shown in Fig. 10 with the constant magnitude 8 for the various values of hypocentral distance. It can be clearly seen that the predominat periods in velocity response spectra become longer as magnitude larger.

The spectral shape by the results mentioned above may be not smooth enough for practical applications. Considering the facts that the coefficients A and B's in the long period range shown in Fig. 8 are nearly constant and those values are nearly equal to the coefficients on magnitude and hypocentral distance of Eq.(2) for maximum velocity respectively, the modified equation for velocity response spectra with damping ratio ξ in addition to the parameters mentioned above is herein proposed as follows:

$$\log Sv(M,X,T,\xi)=0.607M -1.19\log x -1.15 +f1(M,T) -f2(X,T) +f3(\xi,T) \quad (8)$$

Using the correction factors $f3(\xi,T)$ for response spectra with damping ratio ξ derived from the study by Rosenblueth [5], the best fitting trial to the results by Eq.(7) is made on the functions $f1(M,T)$ and $f2(X,T)$. In this trial, the equivalent duration time To of stationary ground motions for the correction factor is defined followingly, making use of the past research [6].

$$To = 10^{0.31M-1.2} \quad \text{in sec.} \quad (9)$$

The final proposal for the smooth velocity response spectra are as follows:

$$f1(M,T) = a_1 x \left(1 - (T/a_2)^{a_3}\right) x \left(1 + T \exp(1 - a_4 T)\right)$$

$$\text{where, } a_1 = 0.015/(M/8)^{14} + 0.055,\ a_2 = 0.045 \times 1.6^{M}$$

$$a_3 = 1.8x(M/8)^{13}/((M/8)^{13} + 0.15),\ a_4 = 0.1/(M/8)^{15} + 0.9 \quad (10)$$

$$f_2(X,T) = 0.25 \times X^{0.1} \times (1/\sqrt{T} - 1)$$

The velocity response spectra with 5% damping by Eq.(8) are illustrated as the dotted lines in Figs.9 and 10, as well.

As for vertical component, spectral characteristics are represented by the mean ratios of velocity response spectra in vertical component to horizontal component for every period, due to the limitation of data. The results calculated from 8 accelerograms are shown in the dotted line of Fig. 8. This result points out the trend that the dominant period of spectrum in vertical component is shorter than that in horizontal component.

In Fig. 11, the velocity response spectra in both horizontal and vertical components for the recorded acceleration at the D1 site of Japan during an earthquake of 1974, and those estimated by the above mentioned procedure are illustrated. In this estimation of response spectra in vertical components, the resulted mean ratios of spectra in Fig. 8 to convert horizontal component into vertical one are applied.

Relation between response spectrum amplification and damping factor

The spectral characteristics of earthquake ground motions proposed in this paper are represented by the velocity response spectra with 5% damping. The response spectra with damping ratio ξ other than 5% in both horizontal and vertical components based on the proposed response spectra with 5% damp-

ing can be obtained by multiplying the amplification coefficients η by the following equation, derived from random vibration theory by response subjected to stationary ground motions with duration To given by Eq.(9) in terms of period T of spectrum.

$$\eta = \begin{cases} 1/\sqrt{1 + 17(\xi - 0.05)\ \exp(-2.5T/To)} & \text{, for } T \geq 0.10 \text{ sec.} \\ 1 & \text{, for } T = 0.02 \text{ sec.} \end{cases} \quad (11)$$

As the background for Eq.(11), the effect of damping factor to response spectral values is analyzed, utilizing 135 horizintal components and 22 vertical components of accelerogram. These values are avaraged in each period, the result of which in horizontal components is shown in Fig.12. As for vertical components, those results are very similar to those in horizontal components. The solid lines in Fig.12 indicate the values of the proposed modification factor in Eq.11 as a parameter of magnitude.

DETERMINISTIC INTENSITY FUNCTION

Figs.13 are the results of efforts to find the deterministic intensity function from the actual accelerograms by smoothing technics of the oscillatory irregular waves. Assuming a(t) is accelerogram, $\zeta(t)$ deterministic intensity function and b(t) is stationary random process of accelerogram, a(t) is expressed;

$$a(t) = \zeta(t)b(t), \qquad b(t) = a(t)/\zeta(t) \quad (12)$$

If real $\zeta(t)$ is to be obtained, b(t) must satisfy the condition of stationary random process such as Gaussian distribution of probability and randomness. Thus true $\zeta(t)$ can be obtained step-by-step smoothing technics through the Run and CHI SQUARE of b(t).

From the shapes of deterministic intensity function, obtained from the 18 sets of strong motion accelerograms in U.S., derived from such checks, the shapes of deterministic intensity function in both horizontal and vertical components (I^h and I^v) can be represented in the following forms;

$$\log I^h(\tau) = 1.08 + 2.13 \times 0.056\tau^{-0.84} - 1.25 \times \tau^{-0.84} - 1.84 \log\tau \quad (13)$$

$$\log I^v(\tau) = 0.81 + 2.22 \times 0.140\tau^{-0.64} - 0.85 \times \tau^{-0.64} - 1.64 \log\tau \quad (14)$$

Where τ is a normalized time (scaled in percentage) obtained by the real time t and the duration time Td; $\tau = 100t/Td$, and then $I(\tau)$ is normalized by the total, that is $\int_0^{100} I(\tau)d\tau = 100$. Accordingly, the shapes of deterministic intensity function in real time can be determined by Eqs.(13) and (14), provided the duration time is given. Figs.14 are the results by Eqs.(13) and (14) with assumption of duration time of 50 seconds, and by smoothing technics of N-S and U-D components of El-Centro 1940.

CONCLUSIONS

On the basis of the analyses of various parameters of earthquake ground motions mentioned in this paper, a procedute to establish the design earthquake may be followingly proposed. The proposal conludes this paper.

Design response spectra

(i) At first, assume magnitude and epicentral distance.
(ii) Estimate the maximum values of acceleration and velocity using Eqs. (1) and (2), then obtain the spectral intensity using linear relations shown in Table 2 in a mean sense.
(iii) Determine the design response spectra using the parameters mentioned

above if response spectrum shape normalized by peak values or spectral intensity is given. If not, one can use the response spectra obtained by Eq.(8). For important structures, one should consider the deviations of parameters such as shown in Table 3.

(iv) Use Eq.(11) in order to convert the response spectra with 5% into those with other dampings.

(v) Use the characteristics of vertical components estimated in this paper such as Eqs.(4), (5) and Fig.8 if necessary.

Time history

(i) Determine the total duration (Td in sec.), in which one can use the following equation[6]

$$\log Td = (M - 2.5)/3.23 \qquad (15)$$

, and the shape of deterministic intensity function by Eqs.(13) and (14).

(ii) Produce the time histories of accelerograms based on the design response spectra.

(iii) Apply the concept of principal axes of earthquake ground motions if multi-dimensional time history ground motions are necessary. The details of this concept are explained in Ref.[7]. Such principal axes satisfy the conditions in which the corresponding variances of motions have maximum, minimum and intermediate values and the covariances equal zero.

(iv) For the comparison of peak accelerations for estimated, calculated and observed ones, the effective peak accelerations are reasonable.

REFERENCES

[1] Housner, G.W., 1959, "Behavior of Structures during Earthquakes", Proc. ASCE, EM4, vol.85, PP.109-129

[2] Kanai, K., 1966, "Improved Empirical Formula for Characteristics of Strong Earthquake Motions", Proc. Japan Earthq. Symp, PP.1-4

[3] Iida, K., 1963, "A Relation of Earthquake Energy to Tsunami Energy and the Estimation of the Vertical Displacement in a Tsunami Source", J. Earthq. Sci. Nagoya Univ., vol. 11, PP.49-67

[4] Kobayashi, H. and Nagahashi, S., 1977, "Response Spectra on Seismic Bedrock during Earthquake", Proc. 6-WCEE, New Delhi.

[5] Rosenblueth, E. and Fustamante, J.E., 1962, "Distribution of Structural Response to Earthquakes", Proc. ASCE, EM3, vol.88, PP.75-106

[6] Hisada, T. and Ando, H., 1973, "On Relationship between Duration and Magnitude of Earthquake Motion at Bedrock", Kajima Inst. Const. Tech.

[7] Penzien, J. and Watabe, M., 1975, "Characteristics of 3-Dimensional Earthquake Ground Motions", Int. J. Earthq. Engng Struct. Dyn., vol.3, PP365-373

Table 1 Coherence among Measures to Represent Intensity of Ground Motion

Y \ X	A	V	D	$SI_{0.0}$	$SI_{0.2}$
A	0.905	0.841	0.587	0.830	0.902
V	0.892	0.798	0.876	0.957	0.986
D	0.739	0.888	0.702	0.826	0.770
$SI_{0.0}$	0.815	0.923	0.786	0.924	0.970
$SI_{0.2}$	0.911	0.960	0.791	0.960	0.897

A half above the diagonal : Horizontal and horizontal
A half below the diagonal : Vertical and vertical
Diagonal matrix : Horizontal and vertical
A : Maximum acceleration V : Maximum velocity
D : Maximum displacement SI_ξ: Housner's intensity
(ξ : Damping ratio)

Table 4 Effective Peak Acceleration

Accelerogram		Peak Acceleration	Effective Peak Acceleration
El Centro	NS	341.	156.
	EW	210.	117.
	UD	206.	92.
Taft	NS	103.	80.
	EW	176.	97.
	UD	79.	35.
Pacoima	NS	1148.	382.
	EW	1055.	352.
	UD	696.	309.
Hachinohe,	NS	225.	163.
	EW	183.	148.
	UD	77.	54.

(gal)

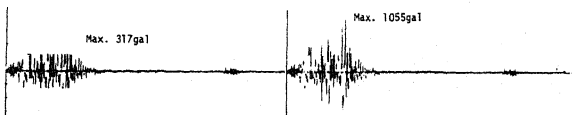

Fig. 6 Cut Out Accelerogram of Pacoima

Fig. 5 Original Accelerogram of Pacoima

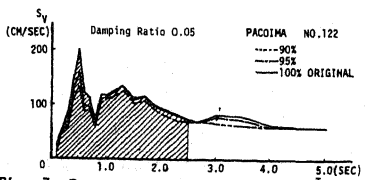

Fig. 7 Response Spectra due to Original and Cut Out Accelerograms of Pacoima

Table 2 Linear Relations between Intensities of Ground Motion

Y \ X	A	V	D	SI 0.0	SI 0.2
A	1.669 (0.532)	0.0961 (8.701)	0.0389 (15.98)	0.579 (1.429)	0.227 (3.945)
V	9.921 (0.0880)	1.753 (0.448)	0.440 (2.000)	5.921 (0.162)	2.242 (0.431)
D	17.67 (0.0406)	1.839 (0.476)	1.555 (0.468)	11.81 (0.0710)	4.290 (0.181)
SI 0.0	1.551 (0.511)	0.157 (5.821)	0.0741 (10.63)	1.887 (0.489)	0.371 (2.610)
SI 0.2	4.819 (0.186)	0.469 (2.035)	0.216 (3.614)	2.855 (0.334)	2.038 (0.435)

H : Horizontal Components
V : Vertical Component
A half above the diagonal : Horizontal and horizontal
A half below the diagonal : Vertical and vertical
Diagonal matrix : Horizontal and vertical
X(row) = coef. Y(column)
Inside parenthesis ; Y(column) = coef. X(row)
example ; $A_H = 1.669 \cdot A_V = 8.701\ V_H$
$A_V = 0.532 \cdot A_H = 9.921\ V_V$

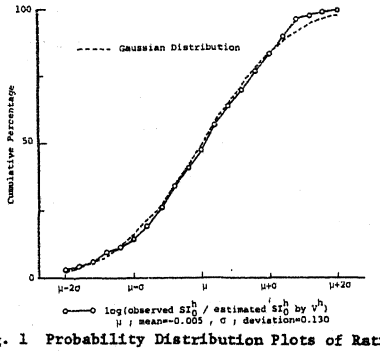

Fig. 1 Probability Distribution Plots of Ratio of Observed Data to Values by Linear Relation

Table 3 Deviations of Ratios of Observed Data to Values by Linear Relations, in Logarithmic Scale

Y \ X	A	V	D	SI 0.0	SI 0.2
A	0.168 (1.472)	0.255 (1.799)	0.369 (2.339)	0.282 (1.914)	0.202 (1.592)
V	0.264 (1.837)	0.104 (1.528)	0.183 (1.524)	0.130 (1.349)	0.128 (1.343)
D	0.366 (2.323)	0.186 (1.535)	0.237 (1.726)	0.245 (1.758)	0.278 (1.897)
SI 0.0	0.271 (1.866)	0.167 (1.469)	0.954 (1.954)	0.135 (1.365)	0.110 (1.288)
SI 0.2	0.206 (1.607)	0.158 (1.439)	0.299 (1.991)	0.100 (1.259)	0.156 (1.432)

A half above the diagonal : Horizontal and horizontal
A half below the diagonal : Vertical and vertical
Diagonal matrix : Horizontal and Vertical
Inside parenthesis : 10 over Deviation

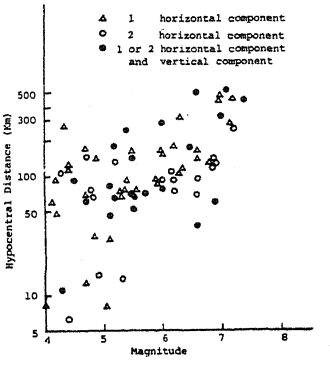

Fig. 2 Relation between Magnitudes and Hypocentral Distances of Data on Rock Sites

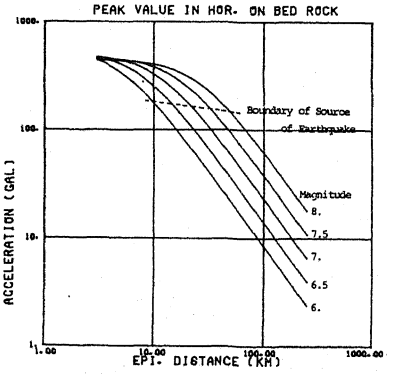

Fig. 3 Maximum Acceleration on Rock Site

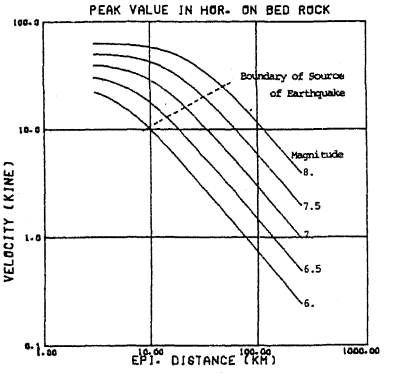

Fig. 4 Maximum Velocity on Rock Site

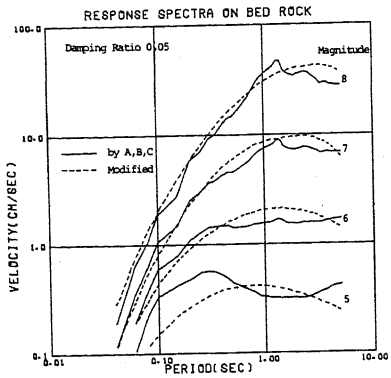

Fig. 9 Velocity Response Spectra on Rock Site at Hypocentral Distance 50km

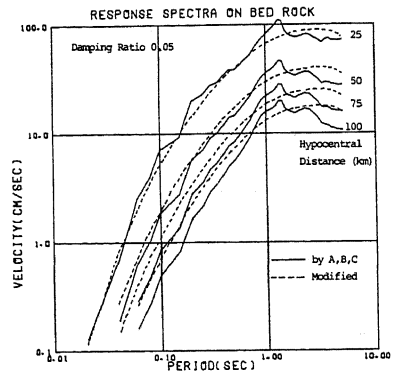

Fig. 10 Velocity Response Spectra on Rock Site at Magnitude 8

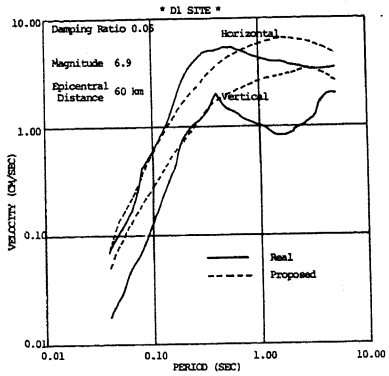

Fig. 11 Comparison between Response Spectra due to Real Earthquake and Calculated Ones

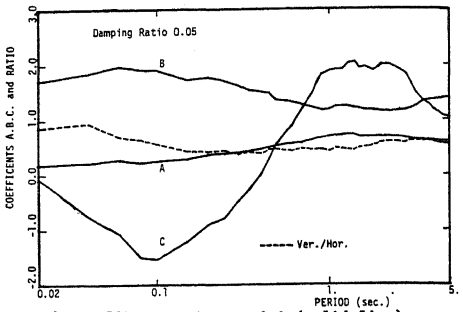

Fig. 8 Coefficients A, B and C (solid line), and Ratios of Response Spectrum in Vertical Component to Horizontal Component (dotted line)

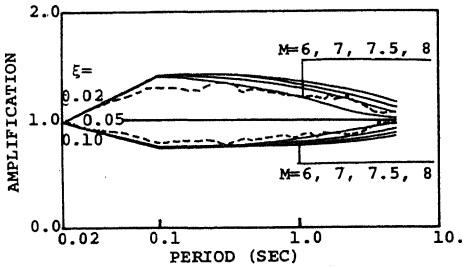

ξ; Damping Ratio
M; Magnitude

Fig. 12 Effect of Damping, Normalized by Response with 5% Damping Ratio

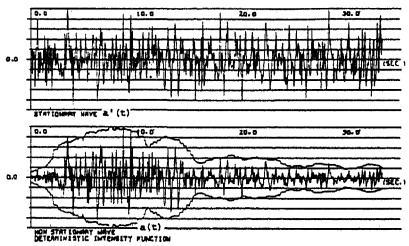

Fig. 13 Deterministic Intensity Function of TAFT-EW

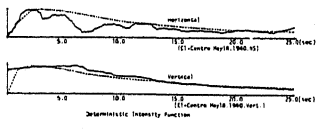

Fig. 14 Comparison between Calculated Deterministic Intensity Functions (dotted line) and Observed Ones (solid line)